Growth and Characterization of Band Gap Engineered InGaAs/InAlAs/GaAs High-electron-mobility Quantum Well Structure Towards Low Leakage VLSI Applications

U. P. Gomes[1*], Y. Chen[2], Y.K. Yadav[1], S. Ghosh[1], S. Chowdhury[1], P. Mukhopadhyay[1], P. Chow[2] and D. Biswas[1]

[1]Advanced Technology Development Center, Indian Institute of Technology Kharagpur, 721302, India
[2]SVT Associates, Eden Prairie, MN 55344, USA
E-MAIL: umeshgomes1@gmail.com, PHONE: +91-9832545359

Abstract

Strained and scaled channel high-mobility quantum well structure has been grown in SVTA MBE for low leakage VLSI applications. Scaling and straining the channel enhances its band gap which is necessary for reducing leakage current. HRXRD confirms the structural quality and strain in the quantum well. Electron mobility is obtained through vander-pauw measurements. Photoluminescence experiments determine the bandgap and the energy level occupancy in the quantum well.

INTRODUCTION

Recent technology roadmap shows that both academia and industries have strong orientation towards InGaAs and other low band gap materials for digital and advanced CMOS applications. Historically, in 1981, a remarkable switching delay of 17.l ps was demonstrated with 0.96 mW power dissipation per gate at 77 K using High Electron Mobility Transistors (HEMTs), and ever since have been desired for LSI applications. A major downfall of III-V in this area was due to high cost, high footprint and immature III-V VLSI processing [1]. According to ITRS, III-V has shown a comeback for digital applications and will stay along with silicon technology. Among III-V materials, GaAs ,and InGaAs are the prime contenders for digital logic applications which require high I_{ON}, very small delay, but at the same time very low leakage especially for low power applications such as mobile platforms. Now even though both the polar semiconductors posses superior transport properties than Si (I_{ON}~ 80% higher for similar dimensions), they trail significantly on terms of leakage ($I_{OFF,Si}$~10^{-13} A/μm compared to $I_{OFF,InGaAs}$~10^{-7} A/μm). As of the two OFF state leakage mechanisms, sub-threshold current which is of great concern with scaling L_g can still be controlled by modifying the applied voltage, the BTBT is only governed by the band gap and tunnel mass. Over the years, InGaAs termed as an emerging research material has been already targeted for logic applications through prototype devices like HEMT, MOS-HEMT, QWFETs and III-V MOSFETs.

InGaAs has an advantage of high mobility with a reported value as high as 10,000 $cm^2V^{-1}s^{-1}$ at sheet carrier density of 3.5 x 10^{12} cm^{-2} [2]. Higher mobility defines the speed of the VLSI ICs. A grand challenge for this alloy semiconductor is its low bandgap. Low band gap means higher power dissipation through gate leakage and tunneling currents, device instability due to impact ionization and high temperature reliability issues. Lowering Indium content towards GaAs rich alloy seems one method for increasing bandgap but this leads to a compromise with mobility and matured material technology of $In_{0.53}Ga_{0.47}As$. A well known method of strain engineering taken from strained silicon technology can be used for bandgap engineering with negligible mobility variation. This technique combined with the advantages of channel quantization can be a solution for low bandgap materials. MBE growth and fabrication technologies help in achieving strained and scaled channels of the order of de Broglie wavelength of carriers in III-V transistors without compromising on the crystal quality. Scaled channels of HEMTs have shown improved logic parameters like DIBL and sub-threshold slope [3].

EXPERIMENTAL DETAILS

The HEMT structure (shown in Table I) consists of 500 nm-thick low-temperature (LT) InAlAs linearly graded to $In_{0.42}Al_{0.58}As$. The starting In composition was set to 0.05 to shorten the growth time. The HEMT structure was grown on epi-ready semi-insulating (100) GaAs substrates by a solid source molecular beam epitaxy equipped with an As valve cracker. Prior to MBE growth, the substrate was heated to a surface temperature of 600 °C to desorb the amorphous oxide layer. 500 nm GaAs buffer was grown at surface temperature of 585 ^{0}C. Then the sample was ramped down for LT-InAlAs growth. Growth rate of AlAs was 0.36 μm/h. The grade of indium content was obtained by increasing the temperature of the indium cell from 600^{0}C to about 830 ^{0}C to reach the In content in $In_xAl_{1-x}As$. To generate a linearly graded buffer layer, the temperature is increased with higher rate at the beginning compared to the end of growth. The growth temperature was 380 ^{0}C for the

LT InAlAs buffer with a V/III beam-equivalent pressure (BEP) ratio of 15. The buffer layer is lattice-mismatched with respect to the InGaAs channel and adds up controlled strain in the channel by tuning the Al mole fraction. It is therefore referred as Strain Transfer Virtual Substrate (STVS) [4]. The 13.5 nm channel is sandwiched between the STVS and barrier layer.

The barrier is modulation doped at n=2×10^{18} cm^{-3}. The channel is maintained at a thickness below the value determined by Matthews-Blakeslee force balance critical thickness model. Furthermore, the 13.5 nm channel is an optimized thickness for having quantization effects at less than half the value of de Broglie wavelength ($\lambda = \frac{h}{\sqrt{3kT\,m_{eff}^*}}$).

A streaky RHEED pattern was observed during the whole MBE growth process. The growth temperatures of HT-InAlAs and subsequent HEMT layers were 480 ^{0}C. All layers in HEMT were grown with minimum As flux necessary to maintain a (2×4) RHEED pattern, which was found to give higher electron mobility for Si-doped epilayers and structures.

TABLE I
LAYOUT OF HIGH-ELECTRON-MOBILITY QUANTUM WELL STRUCTURE

Layer	Thickness (nm)
Si:In$_{0.53}$Ga$_{0.47}$As	6 (2×10^{18} cm^{-3})
Si:In$_{0.42}$Al$_{0.58}$As	10 (2×10^{12} cm^{-2})
In$_{0.42}$Al$_{0.58}$As spacer	7.7
In$_{0.53}$Ga$_{0.47}$As channel	13.5
HT In$_{0.42}$Al$_{0.58}$As STVS	500
LT linear graded In$_x$Al$_{1-x}$As (x=0.05~0.42)	500
GaAs buffer	500
SI-GaAs substrate	

Temperature variant Vander-Pauw Hall measurements were performed on an Accent HL5500 Hall measurement system with optional cryostats in vacuum from 90° K to 500° K with the magnetic field set at 0.5 T. Ohmic contacts to the samples were made by diffusing a small amount of indium through several layers at 300°C in vacuum for approximately 10 min. Crystal quality and strain percentage in the QW has been determined by performing HRXRD. The measurements are performed on Bede D1 Jordan valley HRXRD in double axis configuration with X-ray wavelength of CuK$_{\alpha1}$ radiation. The PL measurements at room temperature were carried out using Accent Photoluminescence setup. The excitation source was 405 nm line of a cube laser (50.0 mW) with InGaAs array detector and monochromator grating of 150 g/mm for maximum spectral resolution.

THEORETICAL DETAILS

Due to the fact that the InGaAs layers are under biaxial compression, this strain splits the light- and heavy-hole states and shifts the band gap to higher energy. The strain-induced band gap shift in conduction band and valence band can be written respectively as:

$$\Delta E_h = [2a\frac{(C_{11}-C_{12})}{C_{11}} + b\frac{(C_{11}+2C_{12})}{C_{11}}]\,\epsilon_\parallel \qquad (1)$$

$$\Delta E_l = [2a\frac{(C_{11}-C_{12})}{C_{11}} - b\frac{(C_{11}+2C_{12})}{C_{11}}]\,\epsilon_\parallel \qquad (2)$$

where a and b are the hydrostatic and uniaxial shear deformation potentials, C_{11} and C_{12} are the elastic stiffness coefficients, and $\epsilon_\parallel$ is the in-plane strain. The calculated strain is -0.0076 considering lattice parameters of InGaAs and InAlAs as 5.8686 and 5.8238 Å respectively. The SQW transition energies for this structure were calculated using a standard Schrodinger-Poisson solutions in TCAD Silvaco [5]. TCAD simulates the Eigen energies and wave functions for both electrons and holes. The bandgap used in the simulation was corrected for the effects of biaxial compressive strain obtained from equations 1 and 2. The material parameters are interpolated from binary values of InAs and GaAs from [6]. Simulated bandgap is 0.8 eV with both effects taken into consideration.

RESULTS AND DISCUSSIONS

Double axis symmetric (004) and asymmetric (224) omega-two theta scan are performed to measure strain in the InGaAs quantum well shown in figure 1. Symmetric (004) Bragg scans were used to measure the lattice parameter in the growth direction (c=6.08243 Å), while the in-plane lattice parameter (a=5.79441 Å) was inferred from the (224)
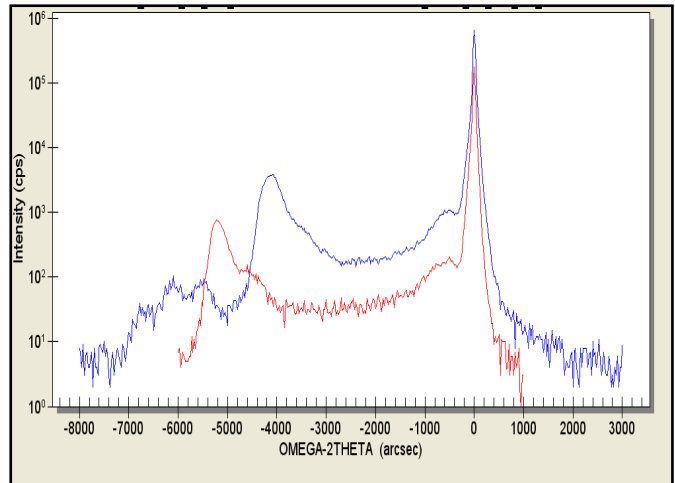

Fig.1. X-ray diffraction rocking curves for the (004) (blue) and the (224) Bragg condition (red) for InGaAs layer on GaAs substrate.

asymmetric reflection. The InGaAs peak shift in the two scans show that the InGaAs QW is tetragonally distorted. The measured strain was -0.0126 considering unstrained lattice constant of InGaAs as 5.8686 Å.

Compressive strain splits the degeneracy of the light hole and the heavy hole which thereby modifies band gap. Energy correction in conduction band and valence band of InGaAs quantum well induced by strain causes a band gap shift of 0.0485 eV calculated from equations 1 and 2. The channel thickness dependent energy gap is obtained by measuring the energy separation between eigen levels in the conduction band and valence band obtained from solving self-consistent coupled Schrodinger-Poisson equations for electrons and holes. The effective energy gap due to the combined effects of strain and channel quantization is calculated from the simulation results. Figure 2 shows the calculated effective energy gap for different channel thicknesses. Theoretical unstrained bandgap is taken as 0.728 eV [7]. No strain model is used as the band gap used in the simulator is strain corrected.
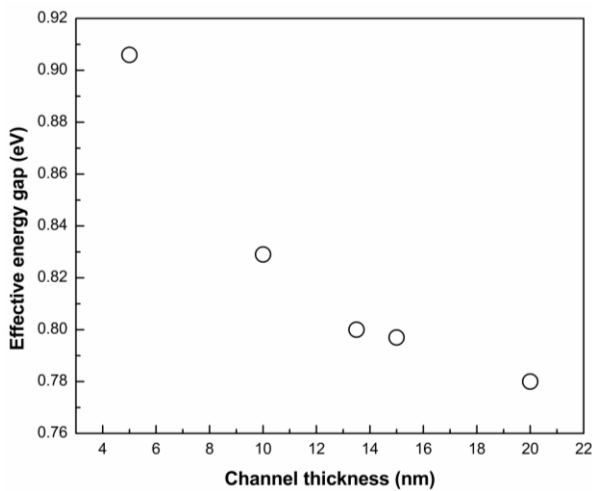

Fig 2: Dependence of effective energy gap on the dimensions of 0.76% compressively strained channel
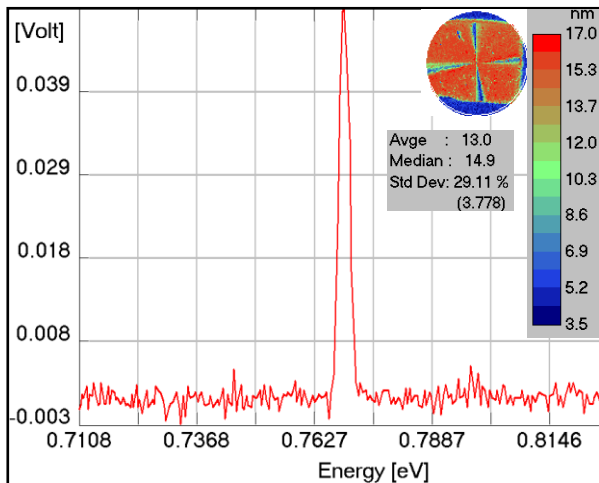

Fig 3: Photoluminescence spectra of 0.76% compressively strained 13.5 nm InGaAs QW

From room temperature photoluminescence measurements (Figure 3) the band gap of the InGaAs QW was obtained as 0.768 eV. As the PL peak of lattice matched InGaAs QW is observed at 0.728 eV [7], it can be inferred that a bandgap enhancement of 0.04 eV (Theoretical calculation gives 0.072 eV) is obtained through scaling and strain engineering the QW through STVS. As the crystalline quality of InGaAs determines the electrical properties of the structure wafer mapping is carried out to measure FWHM. An average of 13 nm shows good crystalline quality.
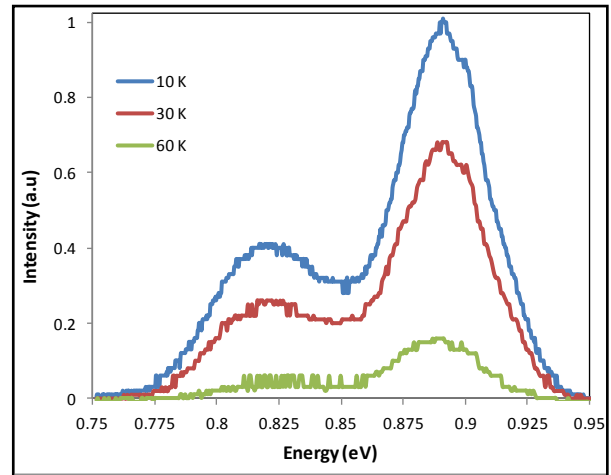

Fig 4: LT Photoluminescence spectra 13.5 nm InGaAs QW showing the second energy level transition.

A low temperature PL experiment shown in Figure 4 confirms double sub-band occupancy. A high intensity PL peak is observed along with the main peak, corresponding to the recombination between the ground-state electronic sub-band (E_2) to the ground-state heavy-hole sub-band (HH_2) transition and E_1 to HH_1 transitions in the InGaAs QW respectively. The identification of these three peaks is supported by simulation results.
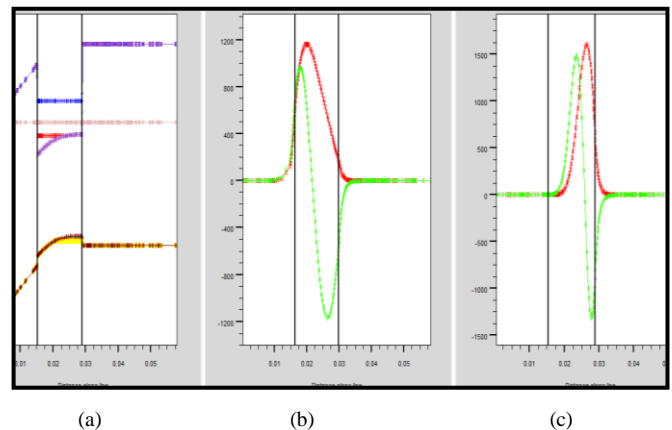

Fig.5: Self Consistent solution of schrodinger-poisson equations to determine the (a) three energy eigen values (b) electron (c) hole wave functions in 13.5 nm InGaAs QW.

Our simulation by self-consistently solving the Schrödinger and Poisson equations to calculate the sub-band energy levels is shown in Figure 5. The simulation shows that two sub-bands are occupied as observed in PL results. The occupancy of second sub-band has major consequences

on device mobility and leakage. The second energy level transition gives a higher recombination probability, and hence, a stronger PL intensity [8]. This can be explained through Figure 5 which shows the asymmetric quantum well edge that reduces overlapping of the electron and hole wave function in the first energy levels. The doping levels are sufficiently high such that the Fermi energy is near the second electron sub-band. Similar structure simulated with lower doping density shows the occupancy of only one energy level [6].

Single occupancy of the first sub-band provides good charge confinement which decreases leakage current by preventing spilling of electrons from the confinement barrier.
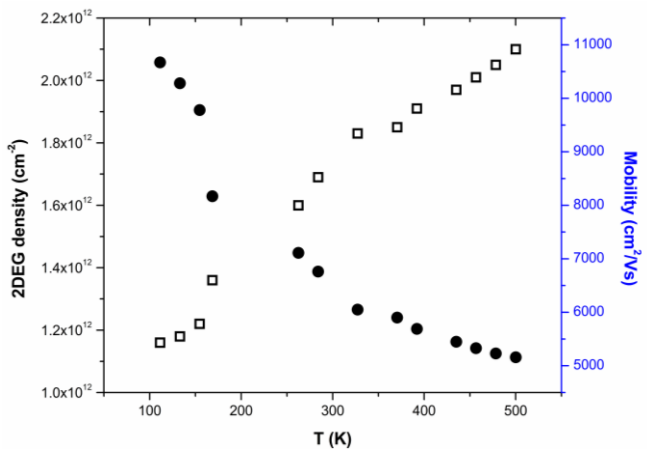

Fig.6: Temperature dependence of the mobility and electron concentration in the InGaAs QW

Hall measurements gives µ=6050±1780 cm^2/Vs at 300 K and maintained similar accuracy limit for HT and LT measurements shown in figure 6. The lower mobility was attributed to the polar optical phonon scattering, inter sub-band scattering, the increase in effective mass due to strain and confinement. It has also been reported that alloy scattering in In$_{0.53}$Ga$_{0.47}$As forms about 20% of the total mobility. The increase in the effective mass due to the electron wave function penetrating into the barrier is negligible as shown in figure 4. The wave functions in the second sub-band penetrate the barrier layer more, and hence the effective mass increases. Our structure appears to be free from this scattering as wave-functions are almost all confined in the InGaAs layer. However, electrons in multiple bands promote inter-band scattering. Temperature dependent Hall measurement shows that mobility decreases rapidly with increasing temperature, as expected for the enhanced polar optical phonon scattering. The phonon scattering is more in this structure because of increase in the phonon frequency due to compressive strain. The product of hall mobility and 2DEG density at ~1.1×10^{18} cm^2/Vs in the entire temperature range promises good thermal stability and electrical stability.

CONCLUSIONS

Devices like HEMTs and III-V MOSFETs that use low bandgap materials in the channel are susceptible to different leakage mechanisms like gate leakage, band to band tunneling and sub-threshold leakage. In order to overcome these "grand challenges" the bandgap needs to be engineered using several techniques. In this work, InGaAs QW high electron mobility transistor structure is grown in solid source MBE with scaled and strained quantum well channel. It is to be noted that we chose InGaAs/InAlAs system over InGaAs /AlGaAs even though the later offers almost similar mobility with much lower In content because we wanted to keep the possibility of introduction of strain by tailoring In content in both the channel and the substrate (SVTS). We expect as the device lengths decreases to less than 10 nm further scaling in both the channel thickness for quantization, and strain induction via tuning the composition of both the channel and barrier layer would be required for device optimization in order to achieve ultimate performance. With Al which has almost constant lattice parameter even with changing Al composition this would never be feasible. We found that scaling the channel to dimensions of de Broglie's wavelength increases the energy levels while straining it causes the bandgap to increase by splitting the heavy hole and the light hole energy levels. Although the structure is strained, Hall measurements confirm that still enough high mobility is retained for high speed applications.

REFERENCES
[1] J. A. Del Alamo, Nature, 479, 317-323 (2012)
[2] S. Datta, et. al., IEEE Electron Device Letters, 28,685-687 (2007)
[3] F. Xue et al., IEEE Electron Device Letters, 33, 1255–1257(2012)
[4] S. Babiker et al., Solid-State Electronics, 43, 1281–1288 (1999).
[5] SILVACO ATLAS manual, Device Simulation Software, SILVACO, Inc., Santa Clara, CA (2011).
[6] U.P. Gomes et al., Current Applied Physics, 13,487-492 (2012)
[7] D. K. Gaskill et al., Appl. Phys. Lett. 56, 1269 (1990)
[8] H. Li et al., J. Appl. Phys.82, 6107 (1997)

ACRONYMS
FWHM: Full Width at Half Maximum
HEMT: High Electron Mobility Transistor
HRXRD: High Resolution X-Ray Diffraction
MBE: Molecular Beam Epitaxy
RHEED: Reflection High Energy Electron diffraction
TCAD: Technology Computer Aided Design
VLSI: Very Large Scale Integration
QW: Quantum Well
QWFET: Quantum Well Field Effect Transistor